Washington University School of Medicine

[Digital Commons@Becker](#)

2005

Targeted deletion of the murine apobec-1 complementation factor (acf) gene results in embryonic lethality

Valerie Blanc
Washington University School of Medicine

Jeffrey O. Henderson
Washington University School of Medicine

Elizabeth P. Newberry
Washington University School of Medicine

Susan Kennedy
Washington University School of Medicine

Jianyang Luo
Washington University School of Medicine

See next page for additional authors

Follow this and additional works at: https://digitalcommons.wustl.edu/open_access_pubs

Please let us know how this document benefits you.

Authors

Valerie Blanc, Jeffrey O. Henderson, Elizabeth P. Newberry, Susan Kennedy, Jianyang Luo, and Nicholas O. Davidson

Molecular and Cellular Biology

Targeted Deletion of the Murine apobec-1 Complementation Factor (*acf*) Gene Results in Embryonic Lethality

Valerie Blanc, Jeffrey O. Henderson, Elizabeth P. Newberry, Susan Kennedy, Jianyang Luo and Nicholas O. Davidson

Updated information and services can be found at:
http://mcb.asm.org/content/25/16/7260

These include:

REFERENCES

This article cites 33 articles, 25 of which can be accessed free
at: http://mcb.asm.org/content/25/16/7260#ref-list-1

CONTENT ALERTS

Receive: RSS Feeds, eTOCs, free email alerts (when new
articles cite this article), more»

Targeted Deletion of the Murine apobec-1 Complementation Factor (*acf*) Gene Results in Embryonic Lethality

Valerie Blanc,[1] Jeffrey O. Henderson,[1] Elizabeth P. Newberry,[1] Susan Kennedy,[1]
Jianyang Luo,[1] and Nicholas O. Davidson[1,2]*

*Division of Gastroenterology, Department of Medicine,[1] and Department of Pharmacology and Molecular Biology,[2]
Washington University School of Medicine, St. Louis, Missouri 63110*

apobec-1 complementation factor (ACF) is an hnRNP family member which functions as the obligate RNA binding subunit of the core enzyme mediating C-to-U editing of the nuclear apolipoprotein B (apoB) transcript. ACF binds to both apoB RNA and apobec-1, the catalytic cytidine deaminase, which then results in site-specific posttranscriptional editing of apoB mRNA. Targeted deletion of *apobec1* eliminates C-to-U editing of apoB mRNA but is otherwise well tolerated. However, the functions and potential targets of ACF beyond apoB mRNA editing are unknown. Here we report the results of generating *acf* knockout mice using homologous recombination. While heterozygous *acf*$^{+/-}$ mice were apparently healthy and fertile, no viable *acf*$^{-/-}$ mice were identified. Mutant *acf*$^{-/-}$ embryos were detectable only until the blastocyst (embryonic day 3.5 [E3.5]) stage. No *acf*$^{-/-}$ blastocysts were detectable following implantation at E4.5, and isolated *acf*$^{-/-}$ blastocysts failed to proliferate in vitro. Small interfering RNA knockdown of ACF in either rat (apobec-1-expressing) or human (apobec-1-deficient) hepatoma cells decreased ACF protein expression and induced a commensurate increase in apoptosis. Taken together, these data suggest that ACF plays a crucial role, which is independent of apobec-1 expression, in cell survival, particularly during early embryonic development.

RNA editing is an important genetic adaptation that permits distinct gene products to be encoded from a single genomic template. One of the most extensively studied examples of this model of mammalian gene regulation is substitutional C-to-U RNA editing of the apolipoprotein B (apoB) transcript, in which a single nucleotide modification results in the translational termination of a truncated protein, apoB48, which is required for intestinal lipid absorption (4). C-to-U editing of the nuclear apoB mRNA is a site-specific deamination reaction that requires a holoenzyme containing a minimal functional core composed of apobec-1, the catalytic deaminase (29), and an RNA binding subunit, apobec-1 complementation factor (ACF) (16, 19). These two proteins interact with one another (16, 19) and also with the substrate apoB RNA (5, 17) in a manner that positions the targeted C residue in an optimal configuration with respect to the active site of the deaminase. Their functional importance and the factors that modulate their respective abundances and subcellular (17) trafficking have been the focus of considerable attention (16, 19, 33).

Studies using recombinant protein and cell extracts have demonstrated that, while necessary for RNA editing, apobec-1 alone is insufficient (23, 26). The requisite importance of apobec-1 was unequivocally revealed through targeted deletion of *apobec1*, which completely eliminated in vivo C-to-U editing of the murine apoB transcript, demonstrating that apobec-1 is an essential and nonredundant component of the holoenzyme (20, 21). Nevertheless, while essential for C-to-U RNA editing, apobec-1 alone is insufficient. In vitro studies using recombi-

nant apobec-1 and ACF have demonstrated that an optimal stoichiometry exists between these two proteins, each of which interacts with one another and with the apoB RNA, notably at a stretch of AU-rich residues flanking the targeted cytidine. Recent work has identified the major functional domains (including three canonical RNA recognition motifs) within ACF that mediate both protein-protein and protein-RNA interaction and that both facilitate and constrain C-to-U RNA editing of the nuclear apoB transcript (5, 17). In addition, ACF contains a novel nuclear localization sequence that directs the importation of heterologous proteins (6). However, while these findings illustrate the range of biochemical mechanisms underlying the role of ACF in apoB RNA editing in vitro, there is little information concerning the requirement for ACF in in vivo RNA editing or the range of alternative or complementary targets, either protein or RNA or both.

In the current study, we have undertaken the targeted deletion of the murine *acf* gene in order to establish the requirement for ACF in C-to-U editing of apoB RNA. Our results from this characterization suggest that ACF has a wider range of targets than apoB RNA alone.

MATERIALS AND METHODS

Generation of *acf*$^{-/-}$ mice. A genomic bacterial artificial chromosome (BAC) clone was obtained by screening a 129/SvJ genomic BAC library (Incyte Genomics) with a full-length mouse ACF cDNA. To replace the exon 2 containing the initiator ATG of ACF with the coding sequence of green fluorescent protein (GFP) and a phosphoglycerol kinase (PGK)-neomycin (Neo) cassette, a replacement-type targeting vector was engineered. To create the 5′ arm, a fragment containing 2.4 kb of DNA upstream of the translation initiation ATG was amplified by PCR with the BAC clone as the template. The GFP "knock-in" cassette was generated by overlapping PCR with the 5′ arm and a GFP amplicon as the templates. The 3-kb 3′ arm was generated by PCR, also with the BAC clone as the template. Both PCR products, i.e., 5′ arm-GFP and the 3′ arm, were subcloned into pGEMT-easy (Promega). Upon digestion with NotI, ApaI, and

* Corresponding author. Mailing address: Washington University School of Medicine, Division of Gastroenterology, Box 8124, 660 S. Euclid Ave., St. Louis, MO 63110. Phone: (314) 326-2027. Fax: (314) 362-2033. E-mail: nod@wustl.edu.

XmnI, the 3′ arm was inserted into the NotI/ApaI sites of p1339 (accession number AF335420; a gift from Tim Ley, Washington University) using restriction sites introduced by PCR. The 5′ arm-GFP cassette was added to the KpnI/BamHI sites of the p1339-3′ arm vector upstream of a PGK-Neo cassette. The targeting construct was linearized with ApaI and electroporated into 129/SvJ embryonic stem (ES) cells. Genomic DNA was isolated from G418-resistant colonies, and correctly targeted clones were identified by Southern blot analysis.

Genotyping analysis. The genotype of ES cells was determined by Southern blotting. Genomic DNA was digested with XbaI, resolved on a 0.8% agarose gel, transferred to a nylon membrane, and hybridized with a ^{32}P-labeled 793-nucleotide (nt) probe corresponding to the sequence downstream of the 3′ arm. Over 140 clones were analyzed for the homologous recombination event. A single positive clone was identified in which a 6.2-kb band was detected in addition to the 8-kb wild-type band. Targeted clones were expanded in culture, and 200 blastocysts were injected into pseudopregnant recipient C57BL/6 mice. A total of three chimeras were obtained, from which two mice were selected for breeding to establish germ line transmission of the targeted allele. The *acf* genotypes were determined by PCR with two different sets of three primers (see Fig. 2A). Set 1 included the following: a sense primer (Sse1), FSPmBAC (5′-CTGAACTGGG AATGAGTGGACATG-3′), was designed from intron 1 to amplify the wild-type and targeted alleles; an antisense primer (ASse1a), mACF Ex2 (5′-CCCCGGA TTTGTGATTTGATT-3′), based on exon 2, will amplify a 338-bp band; and a third primer (ASse1b), GFP90AS (5′-CACGCTGAACTTGTGGCCGTTTAC 3′), corresponding to the GFP sequence, will amplify the targeted allele, producing a 408-bp band. Set 2 included the following: the sense primer (Sse2a), FwdEx2 (5′-ATGGAATCAAATCACAAATCCGGGGATGG-3′), designed from the exon 2, amplifies the wild-type allele producing a 610-bp band; the antisense primer (ASse2), DwnEx2 (5′-CTTTCAAAGGTCTAACATGGGCA GAAGTTG-3′), will amplify both wild-type and targeted alleles; and the third primer (Sse2b), PGK (5′-AGGTGGCGCGAAGGGGCCACCAAAGAACGG-3′), corresponding to the PGK sequence of the Neo cassette, will amplify the targeted allele generating a 230-bp product. *acf*$^{+/-}$ mice were mated and monitored daily for plugs. Embryos at the indicated timed intervals (days postcoitum [dpc]) were recovered by microdissection for histological analysis or genomic DNA extraction with a Puregene DNA purification kit (Gentra Systems) and genotyping as described above.

Protein and RNA extraction and analysis. Tissues were flash frozen in liquid nitrogen and stored at −80°C until used. Protein concentrations were determined (Bio-Rad protein assay) on tissue extracts prior to Western blotting. RNA was isolated using TRIzol (Invitrogen) and 2 μg of DNase-treated RNA used for primer extension analysis of apoB RNA editing and quantitative and semiquantitative reverse transcription (RT)-PCR analysis (7). Real-time quantitative PCRs were performed with an ABI Prism7000 instrument (Applied Biosystems) by use of SYBR Green Master Mix according to the manufacturer's instructions, and mRNA abundance was determined by normalization to the glyceraldehyde-3-phosphate dehydrogenase (GAPDH) level in each sample. PCR primers were as follows: ACF (5′-GCCAGAATCCTGCAATCCA-3′ and 5′-AGCATACCTC TTCGCTTCATCC-3′) and GAPDH (5′-TGTGTCCGTCGTGGATCTGA-3′ and 5′-CCTGCTTCACCACCTTCTTGA-3′). The distribution of ACF mRNA in mouse tissues was assessed by semiquantitative RT-PCR amplification using the following primers: ACF Fwd Ex2 (5′-ATGGAATCAAATCACAATCCGG GGATGG-3′) and antisenseEx7 (5′-CTGGCAGCAGCCTCCGCCTAGCCAT GGCGG-3′). To improve the detection of spliced variants in the tissue survey, PCR was performed using [α-^{32}P]dCTP (3,000 Ci/mmol, 3 μCi/reaction, NEN) as previously described (14). The primers were VBACF17 (5′-CAGCAATTCC CAGTCTTCATTTCC-3′) and VBACF18 (5′-CCCAGGTAAAATGTCATAG AGTTTG-3′). The PCR products were resolved on an 8% polyacrylamide gel electrophoresis (PAGE) gel and analyzed by phosphorimaging. For analysis of promiscuous hyperediting of apoB RNA, a 317-bp sequence of apoB RNA was amplified using primers ND1 (5′-ATCTGACTGGGAGAGACAAGTAGC-3′) and mLiver hypered.rev (5′-CAACAAATAAATAGAGATTATGG-3′). The PCR products were subcloned into PCR-Script (Stratagene) according to the manufacturer's protocol. Ten clones were randomly selected for plasmid DNA isolation and sequencing using an automated sequencer and T3 primer.

siRNA silencing of ACF. Small interfering (siRNA) oligonucleotides were selected following established parameters (11), and several candidate primers, both murine and human specific, were purchased from Dharmacon Research Inc. Rat hepatoma cells (McArdle7777; American Type Culture Collection), a rodent cell line known to express ACF (7, 32), and human hepatoma cells (HepG2) were grown to 40% confluence on coverslips and transfected with 100 nM ACF or control-scrambled siRNA oligonucleotides according to the manufacturer's instructions (Ambion). Forty-eight hours posttransfection, cells were fixed in 10% formalin (Sigma) and probed with a rabbit anti-caspase 3 (active

form) antibody (Cell Signaling) followed by a probe with Cy3 secondary antibody (Jackson Immunoresearch). The nuclei were identified using 4′,6′-diamidino-2-phenylindole (DAPI) (1 mg/ml in phosphate-buffered saline). Silencing of ACF protein expression was also assessed by Western blotting of cell lysates from siRNA or scrambled oligonucleotide-transfected cells grown under identical conditions with a rabbit polyclonal ACF antibody (7).

RESULTS AND DISCUSSION

Murine *acf* gene structure. The murine *acf* gene contains 15 exons with the known functional domains illustrated in Fig. 1A. These findings are generally in agreement with the recent findings of Dur and colleagues (10), with the exception that there are three noncoding exons (exons 5, 6, and 11) reported in the current report (Fig. 1A). The two major protein products (ACF64 and ACF65) differ, as in humans, by the differential splicing of a single exon (Fig. 1A), which results in an eight-amino-acid insertion in the larger protein. A similar pattern of alternative splicing was demonstrated in the human *ACF* gene (14). ACF mRNA expression, as determined by real-time quantitative PCR, was distributed predominantly in the adult liver, small intestine, and kidney (data not shown). This pattern confirms that reported by Dur and colleagues (10). Recombinant human ACF64 and ACF65 reveal indistinguishable biochemical activities (5), but the possibility of an alternative biological function for these isoforms cannot be excluded. ACF43, a splice variant recently described in the rat (26), appears to be a minor transcript (<1%) in murine tissues (data not shown). ACF mRNA and protein were detected at 12 days of mouse embryonic development (Fig. 1B and C). ACF immunostaining was readily detected in the embryonic day 12 (E12) developing heart, spinal cord, and lung tissues (Fig. 1D), in which there is virtually no detectable ACF mRNA or protein in adults (data not shown).

***acf* gene targeting and phenotype characterization following heterozygous deletion.** A replacement-type targeting construct (see Materials and Methods) (Fig. 2A) was electroporated, and ES cells were screened by Southern blotting (Fig. 2B). *acf*$^{+/-}$ ES cells were injected into wild-type blastocysts to create germ line *acf*$^{+/-}$ mice. PCR genotyping (Fig. 2C) was performed to identify mutant mice. *acf*$^{+/-}$ mice appeared healthy, grew at a rate similar to wild-type mice, and were fertile. ACF protein content was reduced in the kidney, liver, and small intestine of *acf*$^{+/-}$ mice relative to that found in wild-type littermates (Fig. 3A).

ACF and apobec-1 interaction yields an enzyme complex whose activity is critically dependent on the stoichiometry of its minimal component subunits (2, 7). To determine the functional consequence of the aforementioned alterations in ACF protein content, we examined the C-to-U editing of endogenous apoB mRNA; the findings demonstrate a consistent and statistically significant increase in the proportions of U$_{6666}$-containing transcripts in both liver and kidney (Fig. 3B). apoB mRNA editing was unchanged in the small intestines of these animals, exceeding 95% in both wild-type and *acf*$^{+/-}$ mice (Fig. 3B). The demonstration of increased apoB mRNA editing in liver and kidney, by contrast, was somewhat unexpected and suggests that heterozygous deletion of ACF alters the stoichiometry of the core components of the holoenzyme. Among the possible considerations in this scenario are alterations in a metabolically active nuclear ACF pool, changes in
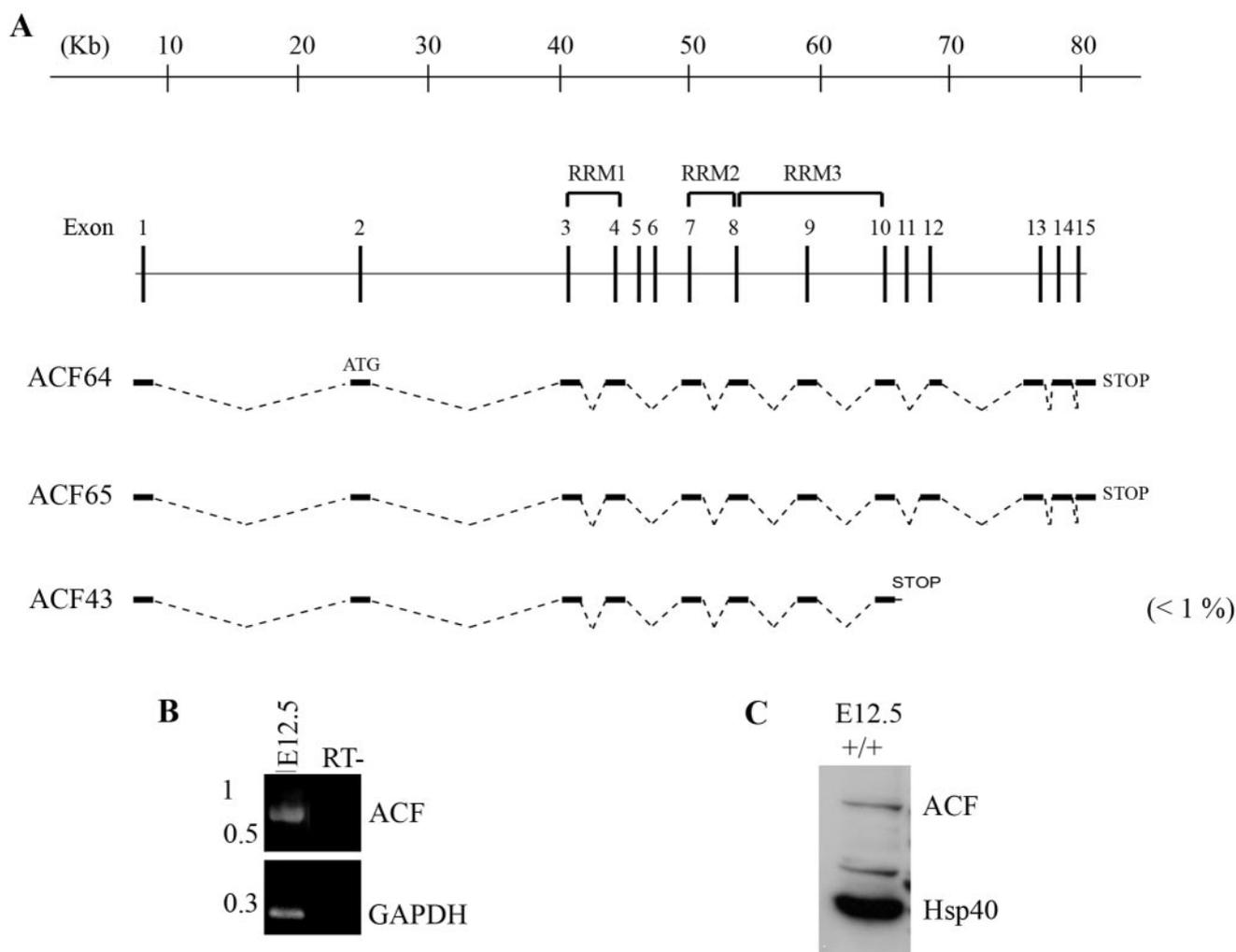
FIG. 1. Genomic organization of the mouse *acf* gene. (A) Upper panel, schematic representation of the intron-exon junctions. Solid bars represent exons. Solid lines represent introns. The exons encoding the three RNA recognition motifs are indicated by brackets. Lower panel, splicing pattern of mouse *acf* gene. (B) Tissue-specific expression of ACF in wild-type mouse embryos. ACF mRNA was extracted from E12.5 embryos and amplified by RT-PCR. The PCR products were resolved on a 1.2% agarose gel and visualized with ethidium bromide. As a positive control, mouse GAPDH RNA was amplified. A negative control performed without reverse transcription is shown (RT−). (C) Protein expression in wild-type embryo. Crude extracts from E12.5 embryos were resolved on a 10% sodium dodecyl sulfate-PAGE gel, transferred to membrane, and probed with antiserum to ACF. (D) ACF expression in an E12.5 embryo. Whole-mount immunostaining of a wild-type embryo at E12.5 with antisera to ACF. Note the staining in heart, lung, and spinal cord. A negative staining performed without primary antibody is shown for each tissue (lower panels).

nuclear cytoplasmic shuttling of apobec-1 and/or ACF (9), or even changes in ACF interaction with other protein partners. These possibilities will of course require formal evaluation in future studies.

In order to determine whether the increased C-to-U editing activity in $acf^{+/-}$ liver was confined to the canonical site at nt 6666, 10 clones were randomly selected from RT-PCR products, and a total of over 3,100 nt sequences was obtained from a region containing eight C residues, including the canonical site (Fig. 3C). The results reveal only one clone (Fig. 3C) in which there was an additional edited C, suggesting that promiscuous editing (25) or hyperediting (31) was not taking place in the setting of increased C-to-U editing at nt 6666. The C-to-U editing of other RNA targets was not examined. Taken together, the functional outcome of the heterozygous targeting

of murine *acf* points to a tissue-specific increase in endogenous apoB RNA editing activity, possibly reflecting a subtle but distinct alteration in the stoichiometry of the core editing complex.

Phenotype associated with homozygous deletion of murine *acf*. Three separate lines of $acf^{+/-}$ mice were established from independent founders, two of which were littermates and one of which was from a separate breeding. The progeny were genotyped by PCR (Table 1). We detected no $acf^{-/-}$ mice from any of these lines after genotyping 42 litters and 332 offspring, indicating that disruption of the *acf* locus resulted in embryonic lethality. The litter sizes from these heterozygous matings were similar to those from wild-type littermates (range, 7 to 10), and there was no apparent gender bias. In addition to the absence of homozygous $acf^{-/-}$ offspring, we
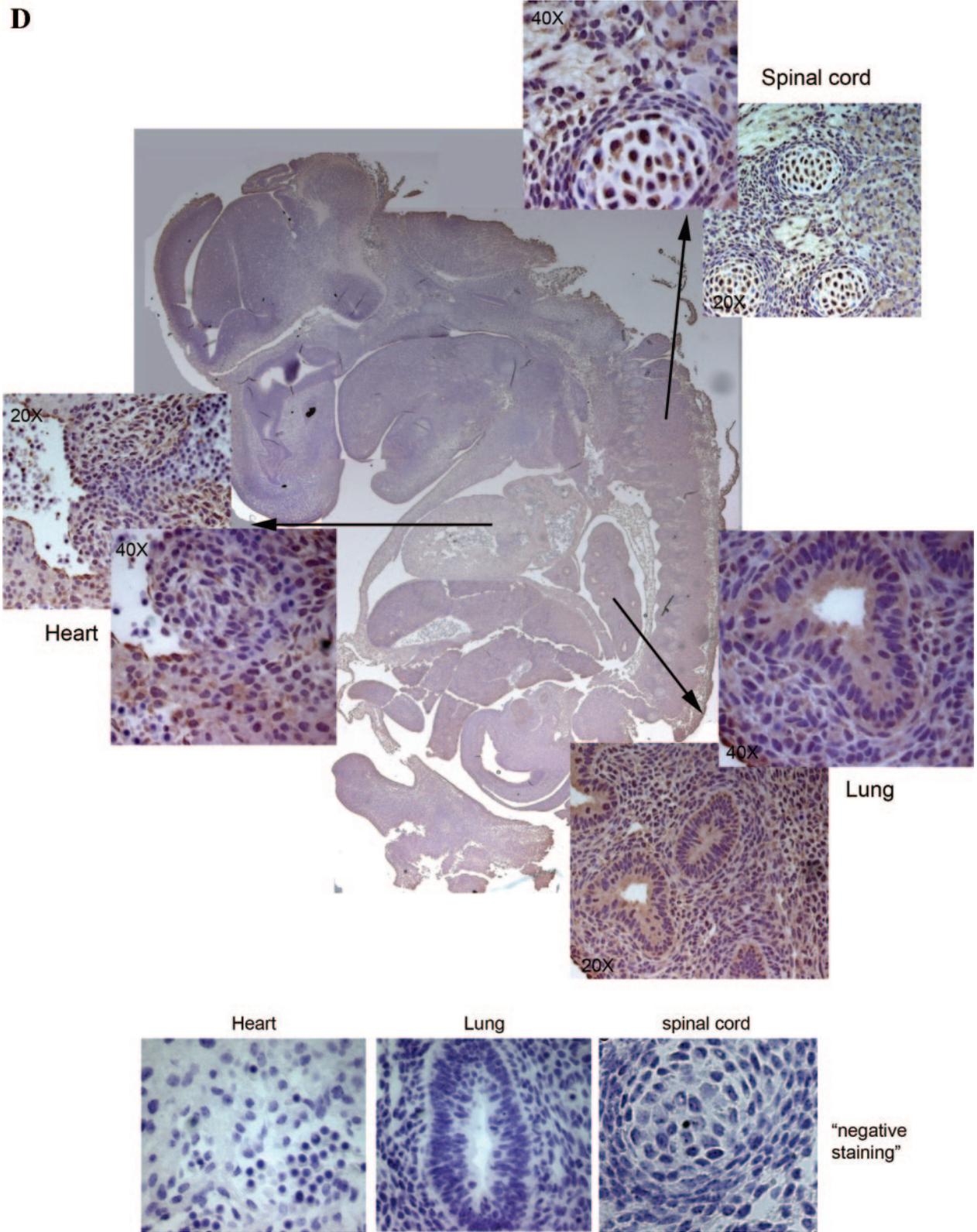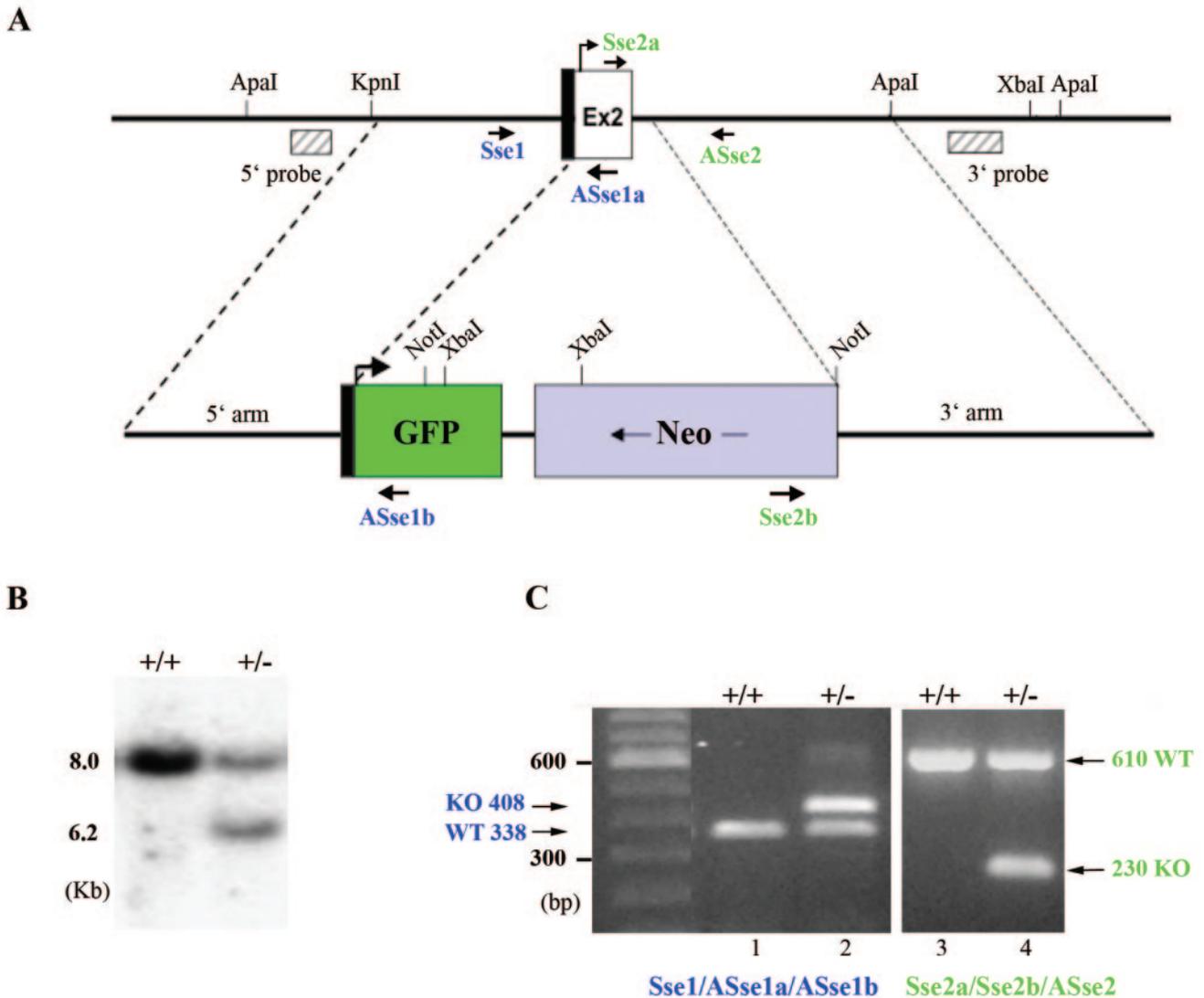
FIG. 1—*Continued*.

FIG. 2. Targeted disruption of *acf* gene. (A) Mouse *acf* gene and targeting vector. Upon homologous recombination of the 5′ and 3′ arms of the targeting vector with the *acf* locus (top), the exon 2 is replaced by the coding sequence of GFP and a LoxP-flanked Neo cassette. (B) Southern blot analysis of genomic DNA isolated from recombinant ES cells. Upon digestion with XbaI, the wild-type (+/+) allele gives rise to a 8-kb fragment, while the digestion of the mutant allele (+/−) generates 8- and 6.2-kb fragments, detected with a 3′ probe (hashed box). (C) PCR genotyping of wild-type and heterozygous mutant mice. Primers Sse1, ASse1a, and Asse1b, indicated in blue, were mixed in a single PCR and used to amplify a 338-bp product corresponding to the wild-type (+/+) and a 408-bp product associated with the targeted allele (+/−), lanes 1 and 2. Similarly, primers Sse2a, Sse2b, and ASse2, indicated in green, amplified a 610-bp wild-type band (lane 3) and a 230-bp band corresponding to the targeted allele (lane 4).

observed a significant increase in heterozygous offspring among all three lines, with the ratio of heterozygous to wild-type mice averaging ~10:1 (range, 8.3 to 12.6) (Table 2), instead of the 2:1 ratio predicted from Mendelian inheritance.

These genotypes were confirmed by two independent primer sets, as detailed in Fig. 2C, suggesting that trivial explanations, such as genotyping errors, are unlikely to account for the apparent increase in the number of heterozygous offspring. In

FIG. 3. Endogenous apoB mRNA editing in wild-type and *acf*^{+/−} mice. (A) Immunodetection of ACF protein in liver, small intestine (SI), and kidney isolated from wild-type or heterozygous mice. Equal amounts of protein were resolved by sodium dodecyl sulfate-PAGE and probed with antisera to ACF, Hsp40, and GFP. (B) apoB mRNA editing of *acf*^{+/−} and wild-type mice. Upper panel, apoB mRNA editing was determined by primer extension. The relative mobility of the unedited (C) and edited (U) products is indicated on the left. Lower panel, bar graph representing the data (mean ± standard deviation; *n* = 4) for each group. Statistically significant differences between groups are indicated by asterisks. (C) Promiscuous editing of hepatic apoB mRNA in *acf*^{+/−} mice. A schematic representation of cytidine residues promiscuously targeted (31) is shown. A 350-bp fragment of apoB mRNA was amplified by RT-PCR, subcloned into pPCR-Script vector, and sequenced. Ten clones from two *acf*^{+/−} mice were analyzed. Nine clones exhibit a uridine residue at the canonical site 6666; only one clone (clone 8) shows an additional C-to-U change at position 6762. Note that a reduction of the ACF protein level does not make the apoB mRNA more susceptible to promiscuous editing.
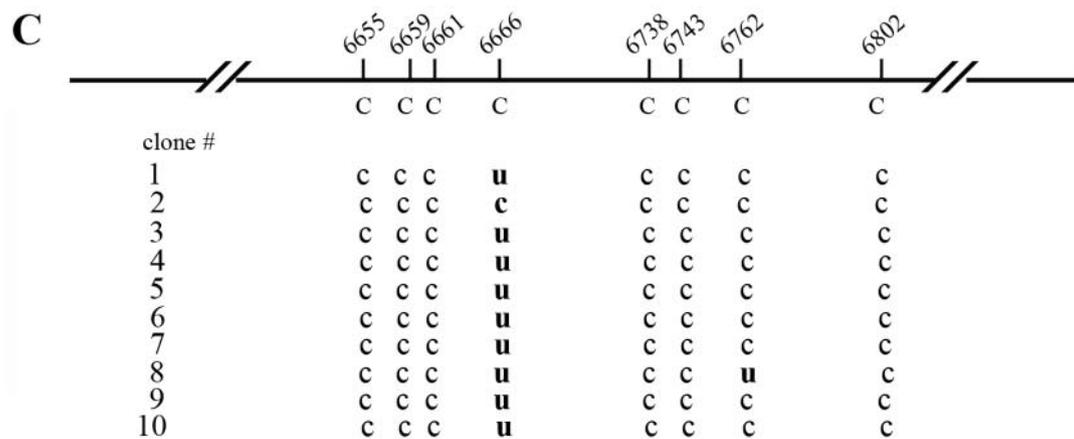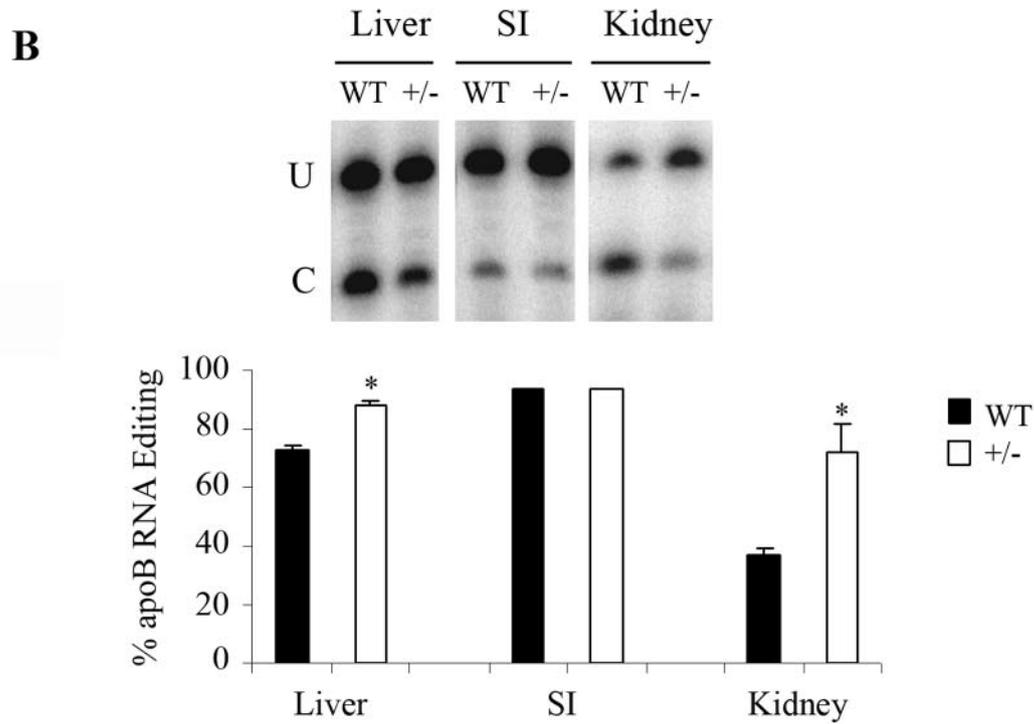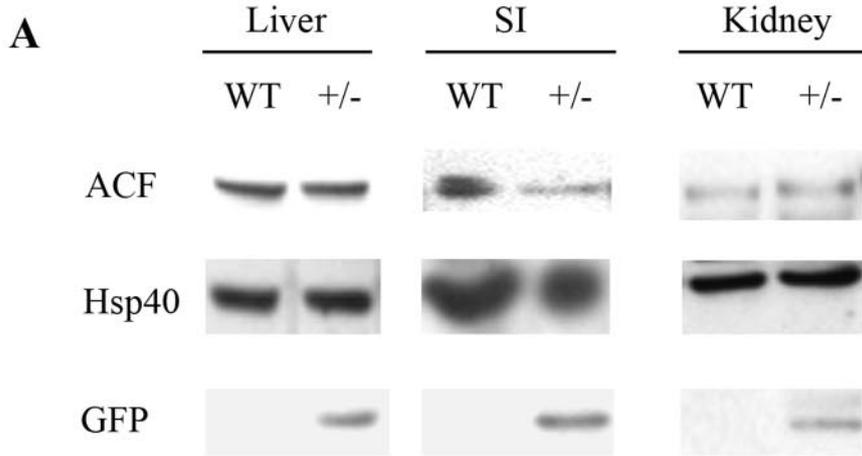
TABLE 1. Numbers of wild-type, heterozygous, and homozygous
null offspring from genotype analysis of progeny from *m acf*
heterozygous intercrosses

Age (dpc)	No. with ACF genotype[a]			Total
	+/+	+/−	−/−	
Weaned	31	301	0	332
12.5	3	14	0	17
7.5	1	16	0	17
3.5	6	27	9	42

[a] +/+, wild type; +/−, heterozygous; −/−, homozygous.

TABLE 2. Details of wild-type and heterozygous *acf* genotype
distribution in each individual line from genotype analysis of
progeny from *m acf* heterozygous intercrosses

Line no.[a]	No. with ACF genotype[b]		het/wt[c]	No. of litters
	+/+	+/−		
1*	13	164	12.6	22
2*	14	117	8.3	16
3	0	20	NA	4

[a] Asterisks indicate lines that were established from two littermate founders.
[b] +/+, wild type; +/−, heterozygous.
[c] het/wt, heterozygous/wild-type ratio; NA, not applicable.

addition, further crosses of the heterozygous $acf^{+/-}$ (mixed background 129/SvJ × C57BL/6) into an *acf* wild-type C57BL/6 $apobec1^{-/-}$ line resulted in two litters containing a total of 12 mice, all of which were $acf^{+/-}$ (data not shown). The karyotype of the targeted ES cells revealed a normal 40 X,Y distribution, suggesting that there is no chromosomal duplication or major rearrangement occurring in the ES cells used to generate the lines. To our knowledge, there are no other examples of an embryonic lethal phenotype where the distribution of genotypes favors the heterozygosity of the candidate gene, but further dissection of the underlying mechanisms will clearly require additional investigation.

To determine the stage at which homozygous mutant mice die, we analyzed embryos at different times of gestation. Genotyping of embryos dissected at E7.5 and E12.5 revealed no $acf^{-/-}$ mice (Table 1). Furthermore, histological examination of the implantation sites ($n = 6$) in uterine sections obtained at E6.5 and E7.5 failed to reveal evidence of thrombi at the positions of putative resorbed deciduae (data not shown). In addition and as expected, no empty deciduae were noted under conditions where all implanted embryos (wild-type and heterozygous $acf^{+/-}$) appeared normal (data not shown). Taken together, these observations suggest that premature death of implanted $acf^{-/-}$ embryos was unlikely to account for the lack of $acf^{-/-}$ mice. We also attempted to recover improperly implanted embryos at E4.5 by flushing the uteri of pregnant $acf^{+/-}$ animals but failed to obtain any material. Taken together, these findings point to an early implantation defect in the $acf^{-/-}$ embryos.

To further investigate the possibility that $acf^{-/-}$ embryos fail to implant, we genotyped 42 blastocysts recovered from the uteri of timed pregnant $acf^{+/-}$ mice at E3.5, a period selected to closely precede implantation. The genotype distribution (Table 1) revealed that 9 were $acf^{-/-}$, 6 were wild type, and 27 were heterozygous $acf^{+/-}$. These results indicate that homozygous $acf^{-/-}$ embryos almost certainly fail to implant.

Among the mechanisms we considered for the failure of $acf^{-/-}$ embryos to implant was an inability to develop properly to the stage where implantation can occur. To assess this possibility, blastocysts (E3.5) were harvested from heterozygous $acf^{+/-}$ mice, cultured for 4 to 7 days, and examined for their ability to develop blastocyst outgrowths (27). The outgrowths were then genotyped by PCR. From 62 cultures, 40 blastocysts remained attached and revealed histological evidence of proliferation of both trophoblasts and inner cell masses (8, 28) (data not shown). Genotype analysis of these 40 outgrowths revealed that 22 were wild type and 18 were heterozygous $acf^{+/-}$. However, no $acf^{-/-}$ outgrowths were detected, consistent with the suggestion that $acf^{-/-}$ blastocysts degenerate and undergo cell death within the first 4 days of culture. These findings collectively point to the possibility that ACF is required for preimplantation development.

ACF knockdown in somatic cells results in apoptotic death. To investigate the possibility that ACF is required for cell survival, we undertook ACF knockdown using siRNA-mediated gene silencing. Rat hepatoma cells were transfected with candidate siRNAs targeting different regions of ACF mRNA (Fig. 4A). ACF protein abundance was reduced by >70%, with siRNAs targeting regions located 316 and 823 nucleotides downstream of the initiator ATG, whereas no effect was observed when cells were transfected with scrambled siRNAs (Fig. 4A). In the setting of ACF knockdown, we observed an increased number of apoptotic cells, as indicated by the number of caspase 3-positive nuclei detected in siRNA4-treated cells (Fig. 4B and D). The initiation of apoptosis was supported by the demonstration of cleavage of caspase 3 into its active form (Fig. 4C). The induction of apoptosis was further analyzed by staining with terminal deoxynucleotidyltransferase-mediated dUTP-biotin nick end labeling. The delivery of siRNA4 to rat hepatoma cells resulted in a significant, approx-

FIG. 4. Silencing of ACF mRNA in McArdle7777 cells. (A) McArdle7777 cells were transfected with individual siRNAs targeting two distinct regions of ACF mRNA. siRNA2 targets a sequence located 316 nt downstream of the transcription initiation codon. siRNA4 recognizes a motif located 823 nt from the ATG. A scrambled siRNA (Sc) was used as negative control. Protein lysates were prepared at 48 h posttransfection, and the ACF level was analyzed by Western blotting using antiserum to ACF. Hsp40 probing was used as the control for equal loading. (B) McArdle7777 cells were transfected with a scrambled siRNA or with siRNA4. At 48 h after transfection, cells were analyzed by immunocytochemistry. For each assay, five fields were analyzed for caspase 3-positive nuclei. The data are representative of three independent experiments. (C) Protein lysates were prepared from McArdle7777 cells transfected with scrambled siRNA or siRNA4. The induction of an apoptotic cascade was analyzed by Western blotting which probed for the active form of caspase 3. An additional control was performed with untreated cells (C). (D) Immunofluorescence microscopy of McArdle7777 cells treated with a scrambled siRNA or siRNA4. Apoptotic cells were characterized by the presence of the active form of caspase 3.
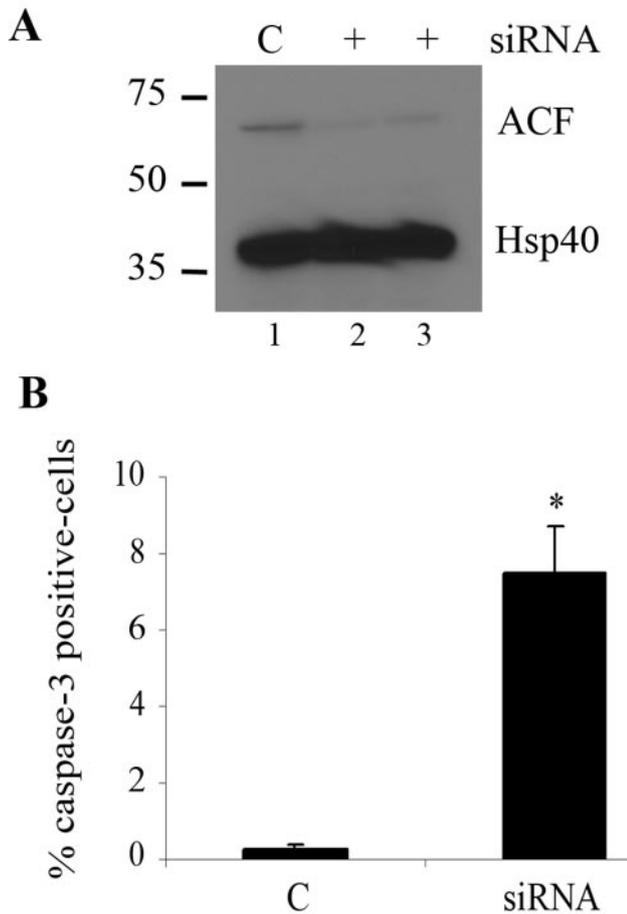
FIG. 5. Silencing of ACF in human hepatoma HepG2 cells. (A) Representative Western blot of ACF protein expression in extracts prepared from HepG2 cells transfected with a human ACF-specific siRNA or a scrambled siRNA control. The Hsp40 signal was used to demonstrate equal protein loading. (B) Quantitative representation of apoptotic cells upon treatment with a scrambled or an ACF-specific siRNA. At 48 h after transfection, HepG2 cells were fixed and stained for caspase 3 (data are means ± standard errors of the means; the asterisk indicates a P value of <0.0002). C, control.

imately threefold increase of the number of nuclei positive by terminal deoxynucleotidyltransferase-mediated dUTP-biotin nick end labeling (~23%) compared to the number in the scrambled siRNA-treated cells (~8%). The induction of apoptosis in rat hepatoma cells was also replicated in experiments using siRNA knockdown of ACF in primary murine hepatocytes (data not shown).

One potential caveat to the conclusions concerning the effects of siRNA-mediated knockdown of ACF expression is that both rat hepatoma cells and murine hepatocytes express both ACF and apobec-1. Since the unconstrained expression of apobec-1 has been shown to be associated with alterations in cellular mRNA stability (1, 3), DNA mutator activity (13, 22), and even altered growth and malignant transformation (3, 30), it was important to extend the findings of siRNA-mediated knockdown of ACF to cells in which no apobec-1 expression is detected. Accordingly, we turned to the human hepatoma HepG2 cell line, since human liver is a robust source of apoB

RNA-editing complementation activity and of ACF expression but does not express apobec-1 (12). siRNA-mediated knockdown of ACF expression in HepG2 cells resulted in an ~76% (four independent assays) decrease in ACF protein expression (Fig. 5A) and a ~30-fold increase in caspase 3-positive-staining nuclei (Fig. 5B). These results reinforce the conclusion that ACF knockdown in somatic cells results in apoptosis. In addition, the findings in HepG2 cells strongly imply that this effect is independent of apobec-1 expression.

To further resolve the observed embryonic lethality associated with homozygous *acf* deletion in vivo, we endeavored to determine the exact timing and cell type in which apoptosis occurs in E3.5 blastocysts. However, as inferred from immunofluorescent staining, ACF expression was below the level of detection in blastocysts isolated from heterozygous *acf* matings, precluding a formal conclusion to the question of whether apoptosis occurs exclusively in *acf* null blastocysts (data not shown). In addition, the transfection of siRNA oligonucleotides into cultured $acf^{+/-}$ ES cells produced inconsistent effects concerning the number of dead and apoptotic cells, which were possibly the result of uncontrolled variations in transfection efficiency (data not shown). We suspect that the resolution of the mechanisms and pathways leading to apoptosis following targeted *acf* deletion will require the development of a conditional deletor line.

Summary conclusions. The central finding of this report is that the homozygous deletion of murine *acf* is associated with embryonic lethality, most likely the result of a developmental defect in blastocyst growth, leading to preimplantation failure. What functional properties of ACF could account for this phenotype? Crucial to its role in catalyzing C-to-U RNA editing is the fact that ACF is an RNA binding protein with high affinity (low k_d) for AU-rich RNAs, including apoB RNA, its presumed target (7, 17, 18). In this regard, it is relevant that several AU-rich RNAs, including those for interleukin-6, interleukin-1β, Cox2, and gamma interferon, are all expressed in the early stages of embryonic development, including the blastocyst stage (24). Although the binding of ACF to these targets has yet to be demonstrated, it is not unreasonable to speculate that altered binding of ACF to any of these or other AU-rich targets might interrupt the development of $acf^{-/-}$ embryos. Probing these underlying mechanisms will require alternative approaches to bypass the early lethality associated with germ line deletion. A potentially important clue to the mechanisms involved in the early embryonic lethality has emerged from recent findings by Kinnaird and colleagues (15). These workers have demonstrated that RNA interference-mediated silencing of the *Caenorhabditis elegans* ACF homolog, HRP-2, leads to embryonic arrest, with 48 h of exposure resulting in a failure to progress beyond the 64-cell stage (15). These findings, considered together with the current data, suggest that ACF is an hnRNP family member with a conserved and nonredundant role in early embryonic development.

REFERENCES

1. **Anant, S., and N. O. Davidson.** 2000. An AU-rich sequence element (UUU N[A/U]U) downstream of the edited C in apolipoprotein B mRNA is a high-affinity binding site for Apobec-1: binding of Apobec-1 to this motif in the 3′ untranslated region of c-*myc* increases mRNA stability. Mol. Cell. Biol. **20:**1982–1992.

2. **Anant, S., J. O. Henderson, D. Mukhopadhyay, N. Navaratnam, S. Kennedy, J. Min, and N. O. Davidson.** 2001. Novel role for RNA-binding protein CUGBP2 in mammalian RNA editing. CUGBP2 modulates C to U editing of apolipoprotein B mRNA by interacting with apobec-1 and ACF, the apobec-1 complementation factor. J. Biol. Chem. **276:**47338–47351.

3. **Anant, S., N. Murmu, C. W. Houchen, D. Mukhopadhyay, T. E. Riehl, S. G. Young, A. R. Morrison, W. F. Stenson, and N. O. Davidson.** 2004. Apobec-1 protects intestine from radiation injury through posttranscriptional regulation of cyclooxygenase-2 expression. Gastroenterology **127:**1139–1149.

4. **Blanc, V., and N. O. Davidson.** 2003. C-to-U RNA editing: mechanisms leading to genetic diversity. J. Biol. Chem. **278:**1395–1398.

5. **Blanc, V., J. O. Henderson, S. Kennedy, and N. O. Davidson.** 2001. Mutagenesis of apobec-1 complementation factor reveals distinct domains that modulate RNA binding, protein-protein interaction with apobec-1, and complementation of C to U RNA-editing activity. J. Biol. Chem. **276:**46386–46393.

6. **Blanc, V., S. Kennedy, and N. O. Davidson.** 2003. A novel nuclear localization signal in the auxiliary domain of apobec-1 complementation factor regulates nucleocytoplasmic import and shuttling. J. Biol. Chem. **278:**41198–41204.

7. **Blanc, V., N. Navaratnam, J. O. Henderson, S. Anant, S. Kennedy, A. Jarmuz, J. Scott, and N. O. Davidson.** 2001. Identification of GRY-RBP as an apolipoprotein B RNA-binding protein that interacts with both apobec-1 and apobec-1 complementation factor to modulate C to U editing. J. Biol. Chem. **276:**10272–10283.

8. **Carlone, D. L., and D. G. Skalnik.** 2001. CpG binding protein is crucial for early embryonic development. Mol. Cell. Biol. **21:**7601–7606.

9. **Chester, A., A. Somasekaram, M. Tzimina, A. Jarmuz, J. Gisbourne, R. O'Keefe, J. Scott, and N. Navaratnam.** 2003. The apolipoprotein B mRNA editing complex performs a multifunctional cycle and suppresses nonsense-mediated decay. EMBO J. **22:**3971–3982.

10. **Dur, S., K. Krause, N. Pluntke, and J. Greeve.** 2004. Gene structure and expression of the mouse APOBEC-1 complementation factor: multiple transcriptional initiation sites and a spliced variant with a premature stop translation codon. Biochim. Biophys. Acta **1680:**11–23.

11. **Elbashir, S. M., J. Harborth, K. Weber, and T. Tuschl.** 2002. Analysis of gene function in somatic mammalian cells using small interfering RNAs. Methods **26:**199–213.

12. **Giannoni, F., D. K. Bonen, T. Funahashi, C. Hadjiagapiou, C. F. Burant, and N. O. Davidson.** 1994. Complementation of apolipoprotein B mRNA editing by human liver accompanied by secretion of apolipoprotein B48. J. Biol. Chem. **269:**5932–5936.

13. **Harris, R. S., S. K. Petersen-Mahrt, and M. S. Neuberger.** 2002. RNA editing enzyme APOBEC1 and some of its homologs can act as DNA mutators. Mol. Cell **10:**1247–1253.

14. **Henderson, J. O., V. Blanc, and N. O. Davidson.** 2001. Isolation, characterization and developmental regulation of the human apobec-1 complementation factor (ACF) gene. Biochim. Biophys. Acta **1522:**22–30.

15. **Kinnaird, J. H., K. Maitland, G. A. Walker, I. Wheatley, F. J. Thompson, and E. Devaney.** 2004. HRP-2, a heterogeneous nuclear ribonucleoprotein, is essential for embryogenesis and oogenesis in Caenorhabditis elegans. Exp. Cell Res. **298:**418–430.

16. **Lellek, H., R. Kirsten, I. Diehl, F. Apostel, F. Buck, and J. Greeve.** 2000. Purification and molecular cloning of a novel essential component of the apolipoprotein B mRNA editing enzyme-complex. J. Biol. Chem. **275:**19848–19856.

17. **Mehta, A., and D. M. Driscoll.** 2002. Identification of domains in apobec-1 complementation factor required for RNA binding and apolipoprotein-B mRNA editing. RNA **8:**69–82.

18. **Mehta, A., and D. M. Driscoll.** 1998. A sequence-specific RNA-binding protein complements apobec-1 to edit apolipoprotein B mRNA. Mol. Cell. Biol. **18:**4426–4432.

19. **Mehta, A., M. T. Kinter, N. E. Sherman, and D. M. Driscoll.** 2000. Molecular cloning of apobec-1 complementation factor, a novel RNA-binding protein involved in the editing of apolipoprotein B mRNA. Mol. Cell. Biol. **20:**1846–1854.

20. **Morrison, J. R., C. Paszty, M. E. Stevens, S. D. Hughes, T. Forte, J. Scott, and E. M. Rubin.** 1996. Apolipoprotein B RNA editing enzyme-deficient mice are viable despite alterations in lipoprotein metabolism. Proc. Natl. Acad. Sci. USA **93:**7154–7159.

21. **Nakamuta, M., B. H. Chang, E. Zsigmond, K. Kobayashi, H. Lei, B. Y. Ishida, K. Oka, E. Li, and L. Chan.** 1996. Complete phenotypic characterization of apobec-1 knockout mice with a wild-type genetic background and a human apolipoprotein B transgenic background, and restoration of apolipoprotein B mRNA editing by somatic gene transfer of Apobec-1. J. Biol. Chem. **271:**25981–25988.

22. **Petersen-Mahrt, S. K., and M. S. Neuberger.** 2003. In vitro deamination of cytosine to uracil in single-stranded DNA by apolipoprotein B editing complex catalytic subunit 1 (APOBEC1). J. Biol. Chem. **278:**19583–19586.

23. **Richardson, N., N. Navaratnam, and J. Scott.** 1998. Secondary structure for the apolipoprotein B mRNA editing site. AU-binding proteins interact with a stem loop. J. Biol. Chem. **273:**31707–31717.

24. **Rothstein, J. L., D. Johnson, J. A. DeLoia, J. Skowronski, D. Solter, and B. Knowles.** 1992. Gene expression during preimplantation mouse development. Genes Dev. **6:**1190–1201.

25. **Siddiqui, J. F., D. Van Mater, M. P. Sowden, and H. C. Smith.** 1999. Disproportionate relationship between APOBEC-1 expression and apolipoprotein B mRNA editing activity. Exp. Cell Res. **252:**154–164.

26. **Sowden, M. P., D. M. Lehmann, X. Lin, C. O. Smith, and H. C. Smith.** 2004. Identification of novel alternative splice variants of APOBEC-1 complementation factor with different capacities to support apolipoprotein B mRNA editing. J. Biol. Chem. **279:**197–206.

27. **Stopka, T., and A. I. Skoultchi.** 2003. The ISWI ATPase Snf2h is required for early mouse development. Proc. Natl. Acad. Sci. USA **100:**14097–14102.

28. **Tanaka, Y., N. P. Patestos, T. Maekawa, and S. Ishii.** 1999. B-myb is required for inner cell mass formation at an early stage of development. J. Biol. Chem. **274:**28067–28070.

29. **Teng, B., C. F. Burant, and N. O. Davidson.** 1993. Molecular cloning of an apolipoprotein B messenger RNA editing protein. Science **260:**1816–1819.

30. **Yamanaka, S., M. E. Balestra, L. D. Ferrell, J. Fan, K. S. Arnold, S. Taylor, J. M. Taylor, and T. L. Innerarity.** 1995. Apolipoprotein B mRNA-editing protein induces hepatocellular carcinoma and dysplasia in transgenic animals. Proc. Natl. Acad. Sci. USA **92:**8483–8487.

31. **Yamanaka, S., S. Poksay, D. M. Driscoll, and T. L. Innerarity.** 1996. Hyperediting of multiple cytidines of apolipoprotein B mRNA by APOBEC-1 requires auxiliary protein(s) but not a mooring sequence motif. J. Biol. Chem. **271:**11506–11510.

32. **Yang, Y., N. Ballatori, and H. C. Smith.** 2002. Apolipoprotein B mRNA editing and the reduction in synthesis and secretion of the atherogenic risk factor, apolipoprotein B100 can be effectively targeted through TAT-mediated protein transduction. Mol. Pharmacol. **61:**269–276.

33. **Yang, Y., and H. C. Smith.** 1997. Multiple protein domains determine the cell type-specific nuclear distribution of the catalytic subunit required for apolipoprotein B mRNA editing. Proc. Natl. Acad. Sci. USA **94:**13075–13080.